Crack Propagation in Polymer Adhesive/Glass Sandwich Specimens

J. E. Ritter[a]; T. J. Lardner[a]; A. J. Stewart[a]; G. C. Prakash[a]

[a] Department of Mechanical Engineering, University of Massachusetts, Amherst, Massachusetts, USA

PLEASE SCROLL DOWN FOR ARTICLE

Crack Propagation in Polymer Adhesive/Glass Sandwich Specimens

J. E. RITTER, T. J. LARDNER, A. J. STEWART and G. C. PRAKASH

Department of Mechanical Engineering, University of Massachusetts, Amherst, Massachusetts 01003, USA

Moisture-assisted crack growth in polymer adhesive/glass interfaces was measured as a function of the applied energy release rate, G, using a four-point flexure test coupled with an inverted microscope. The specimens consisted of two glass plates bonded together with an epoxy or an epoxy-acrylate adhesive. It was found that cracks formed and grew on both interfaces if the glass surfaces were both smooth; however, roughening the surface of one of the glass plates increased the fracture resistance of the interface sufficiently so that crack growth occurred only on the remaining "smooth" interface (top or bottom). Finite element analysis was used to determine the G and ψ (phase angle) appropriate for the different crack geometries. It was found experimentally that crack growth rates for all crack geometries depended on the applied G via a power law relationship and that for a given applied G, crack growth rates were sensitive to the crack geometry. The results indicate that the primary driving force for moisture-assisted crack growth at a polymer/glass interface is the applied G at the crack tip and that the effect of the phase angle for the different crack geometries (13° to 54°) is negligible.

KEY WORDS: polymer adhesion; epoxy/glass; crack propagation; interfacial failure; moisture-assisted crack growth; interfacial fracture resistance

INTRODUCTION

Polymer adhesives are widely used in the electronic and optical industries as coatings to protect glass surfaces and as interlayers to bond two plates of glass together. Preventing delamination of the polymer/glass interface is of critical importance to the successful application of these polymer adhesive. Interfacial failure can occur when the energy release rate, *i.e.* the driving force, for interfacial crack growth reaches a critical value (G_c) or when environmental factors such as moisture causes slow crack growth at an energy release rate G less than G_c. Environmentally-assisted crack growth is most important from a design standpoint since crack growth can occur at a relatively low G and can lead to a delayed failure. It is moisture-assisted crack growth at polymer/glass interfaces that is the focus of this research.

In previous research,[1,2] we found from fracture tests of glass/polymer/glass specimens that cracks on the interfaces can propagate in several different ways. If both polymer/glass interfaces have equal fracture resistance, then cracks form and propagate on both interfaces of the sandwich specimen. On the other hand, if one of the interfaces is weaker, then crack propagation will be solely on the weak interface. The

purpose of the present research is to study in detail moisture-assisted crack growth and the choice of interface in glass/polymer/glass sandwich specimens. The polymer adhesives studied were epoxy and epoxy acrylate. Finite element analysis was carried out to gain a better understanding of the observed crack.growth behavior.

EXPERIMENTAL PROCEDURE

The sandwich specimen, see Figure 1, consisted of two clean, annealed glass plates (about $40 \times 8 \times 1$ mm) bonded together with an epoxy adhesive (DGEBA, Devcon Corp.) or an epoxy acrylate adhesive (950-008 DSM Desotech, Inc). These specimens were made by pressing the glass plates between two blocks that had stops set to control the thickness of the adhesive layer to $40 \mu m \pm 15 \mu m$. The manufacturers' recommendations were followed to cure both the epoxy for 24 h in ambient air and the epoxy acrylate under ultraviolet light for 24 h. After curing, the edges of the specimens were polished (240 grit abrasive paper) to eliminate any excessive adhesive that had squeezed out between the plates.

To limit crack formation and growth to one interface, one of the glass plates was abraded (mean roughness about 3 μm) on one side. This roughened interface increased the fracture resistance of the interface sufficiently so that crack formation and growth on this interface was inhibited. Thus, with this technique we could initiate and grow a crack entirely along either interface #1 or #2 (whichever was the "smooth" interface) without a crack on the other interface, see Figure 2. Note that for a crack on interface #2, the adhesive ligament remains intact between the initial, precrack in the glass plate and the interfacial crack. When both glass surfaces were smooth (mean roughness about 0.05 μm), cracks would form and grow on both interfaces simultaneously.

A four-point flexure test[1] was used to study moisture-assisted crack growth along the epoxy/glass interfaces. Figure 3 shows a schematic of the apparatus that was constructed to fit on the stage of an inverted optical microscope (Zeiss IM35). The inner and outer spans were 22.23 and 31.75 mm, respectively. A button load cell (Sensotec Model 53) was used in conjunction with a digital multimeter (Keithley 175) to record the
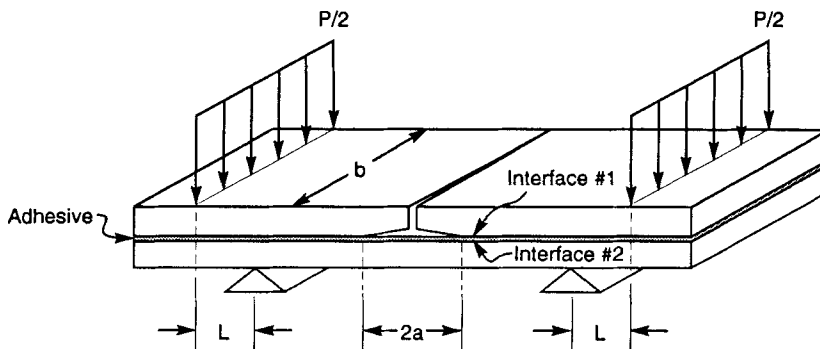

FIGURE 1   Schematic of the interfacial, four-point flexure sandwich specimen.
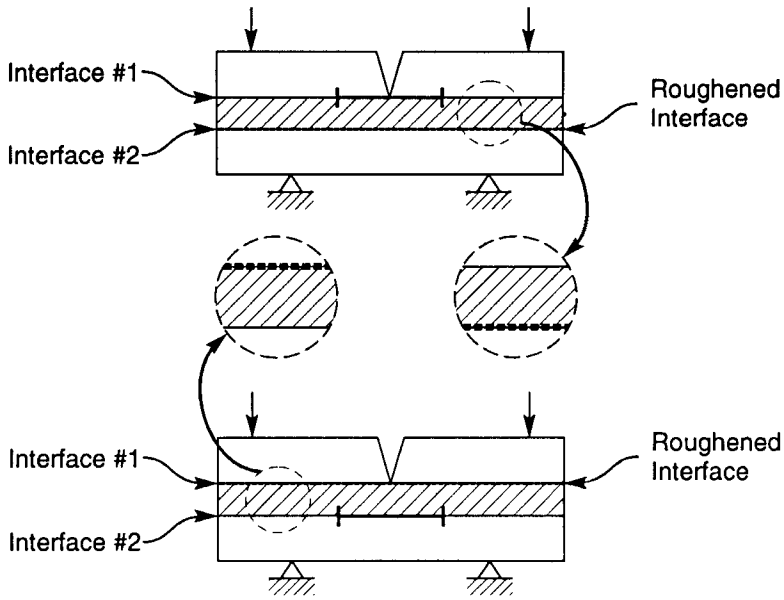
FIGURE 2   Schematic of crack confined to interface #1 or #2 in the sandwich specimen.
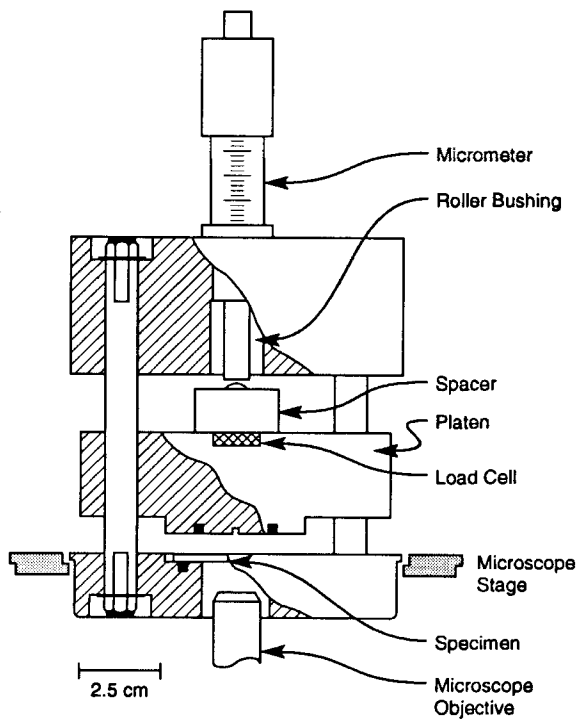
FIGURE 3   Schematic of the interfacial, four-point flexure apparatus.

applied load. The load was applied to the specimen by turning the micrometer. This apparatus was used both to precrack the specimen and to measure moisture-assisted crack growth as a function of time at a given applied load. Precracking was achieved by placing several Vickers indentation cracks (indent load $= 30\,N$) along the width of the top glass plate. Upon loading the sample in 3-point bending with the indented surface on the tensile side, a crack propagated from the array of indents to interface # 1 and then a crack would form symmetrically in the "smooth" interface (# 1, # 2, or both). It is important to note that when cracks appeared on interface # 2, the adhesive always remained intact, *i.e.* a crack never ran through the polymer adhesive.

The precracked specimens were preconditioned for 24 h at a high humidity by storing them in a bell jar with a saturated aqueous salt solution to give the test humidity of 75–80%. This was done to ensure that each specimen was equilibrated to the high humidity before testing. The preconditioned specimens were then placed into 4-point bending with the precracked side in tension and the interfacial crack tips within the inner loading span. Crack growth at a given applied load was monitored with the microscope. It should be noted that to maintain constant load during the test, the micrometer screw had to be periodically adjusted. The interfacial crack produced an interference pattern due to the gap separating the crack surfaces that allowed it to be easily observed. All crack growth experiments were carried out at 75–80% relative humidity by enclosing the fixture in a plastic envelope and then piping into the envelope saturated nitrogen gas.

For an applied load, P, and a thin adhesive layer, the applied energy release rate, G, for a crack only on interface # 1 is given by:[3,4]

$$G = \frac{(PL)^2}{8Eb}\left[\frac{1}{I_2} - \frac{1}{I_c}\right] \tag{1}$$

where b is the sample width, E is the elastic modulus of the glass, I_2 and I_c are the moments of inertia of the lower glass plate and composite specimen, respectively. Note that G is independent of the crack length for cracks within the inner loading span. For this sandwich flexure specimen, the phase angle (a measure of the shear to tensile stress at the crack tip) is about $30°$ for a crack solely on interface # 1.[4] Note that increasing the shear stress at the crack tip, *i.e.* increasing phase angle, tends to drive the crack out of the interface.

RESULTS AND DISCUSSION

A. Crack Formation and Growth Observations

For specimens that had both interfaces "smooth", the indent crack would diverge into interface # 1 and then cracks at the edges on interface # 2 would tend to form near the leading front of the crack on interface # 1 and grow across the width of the specimen either during precracking or during the moisture-assisted crack growth experiments. However, this dual cracking phenomenon was much more prevalent with the epoxy specimens (over 80% of the samples) than with the epoxy-acrylate specimens (less than 30%). Consequently, in these sandwich samples where both glass interfaces were

"smooth", the crack growth data presented herein for the epoxy specimens are for cracks growing on interface #2 in the presence of a crack on interface #1, while for the epoxy-acrylate specimens the crack growth data are for a crack that formed and grew solely on interface #1. Figure 4 illustrates how two cracks initiated from the edges of an epoxy specimen on interface #2 and grew across the width of the specimen during the 4-point flexure test to form a fully-developed crack on interface #2. Note that the edge cracks on interface #2 as they grew across the width of the sample advance forward at about the same rate as the crack on interface #1. Once the edge cracks on interface #2 had propagated entirely across the width of the sample, the now fully-developed crack on interface #2 propagated forward at a linear rate while the original crack on interface #1 arrested. Thus, for this dual crack geometry, crack growth rates for the crack on interface #2 were measured after the edge cracks had grown across the width of the sample and the crack on interface #1 had arrested. Figure 5 shows a typical cross-sectional view of an epoxy sample with cracks on both interfaces. Note that the epoxy adhesive remains intact between the cracks on the two interfaces and that the crack on
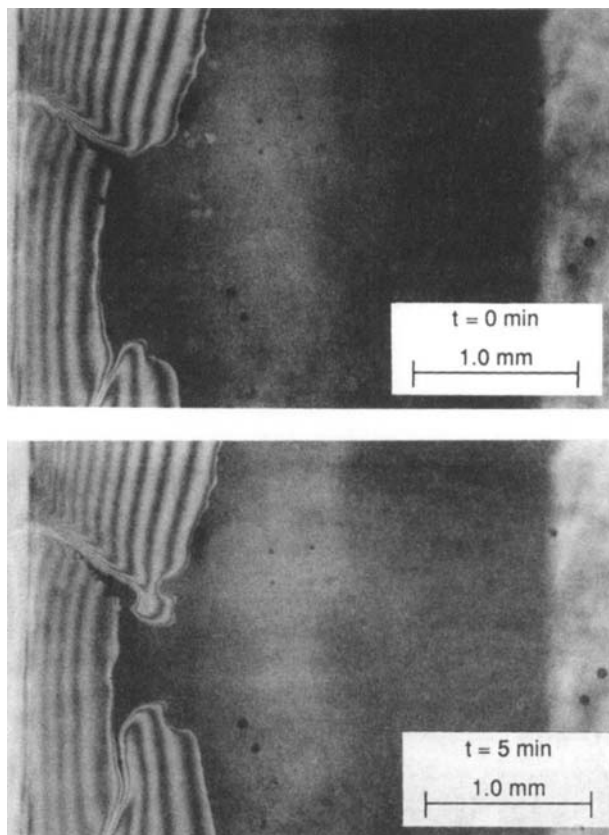

FIGURE 4   Sequence of micrographs showing the linking up of two cracks on interface #2 at 75–80% RH and $G = 3.4$ J/m^2.
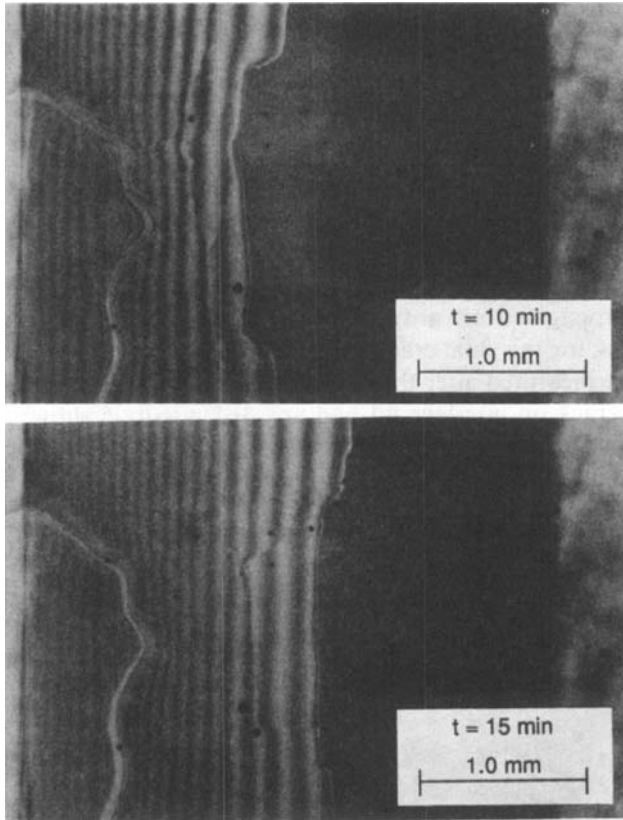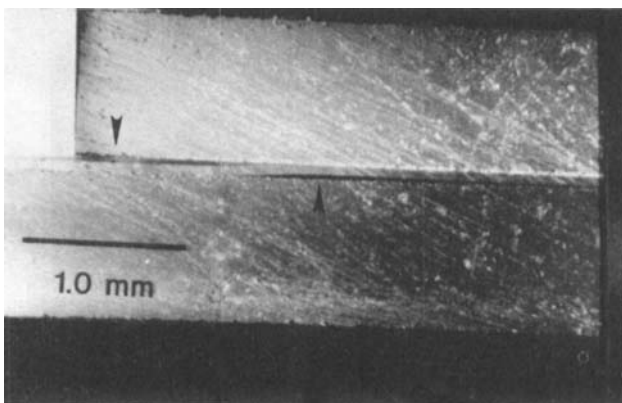
FIGURE 4   (*Continued.*)

FIGURE 5   Cross section of a sample with cracks on both interfaces (see arrows).

interface #2 only runs partially underneath the crack on interface #1 creating an overlap between the tips of the cracks on interface #1 and #2 of about 5–10 times the thickness of the adhesive.

For both epoxy and epoxy-acrylate specimens where cracks formed and grew exclusively on interface #1, the crack length varied linearly with respect to time, see Figure 6. However, for specimens where cracks formed and grew solely on interface #2, crack growth was generally characterized, especially at the lower applied energy release rates, by an intermittent "stop-go" action where the crack would arrest then suddenly propagate forward before assuming a linear growth rate. This "stop-go" crack growth sequence would repeat itself several times during the experiment, see Figure 7. In these cases the average crack growth rate, V, over the time span of the experiment was calculated.

For all crack geometries a threshold value of G was observed where below this threshold G no crack growth was observed in the time span of the experiment (up to 64 h). In some cases, especially for cracks exclusively on interface #2, the crack would actually recede somewhat, see Figure 8. Note in Figure 8 that a light fringe corresponding to the position where the crack tip initially arrested is still visible after the crack closed up.
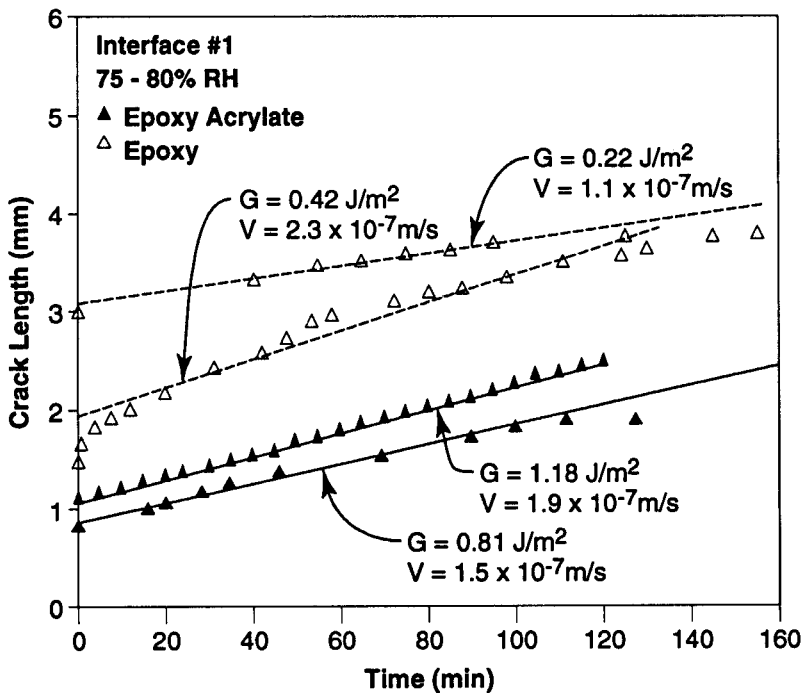
FIGURE 6   Crack length *versus* time for epoxy and epoxy-acrylate/glass sandwich specimens where cracks formed and grew solely on interface #1.
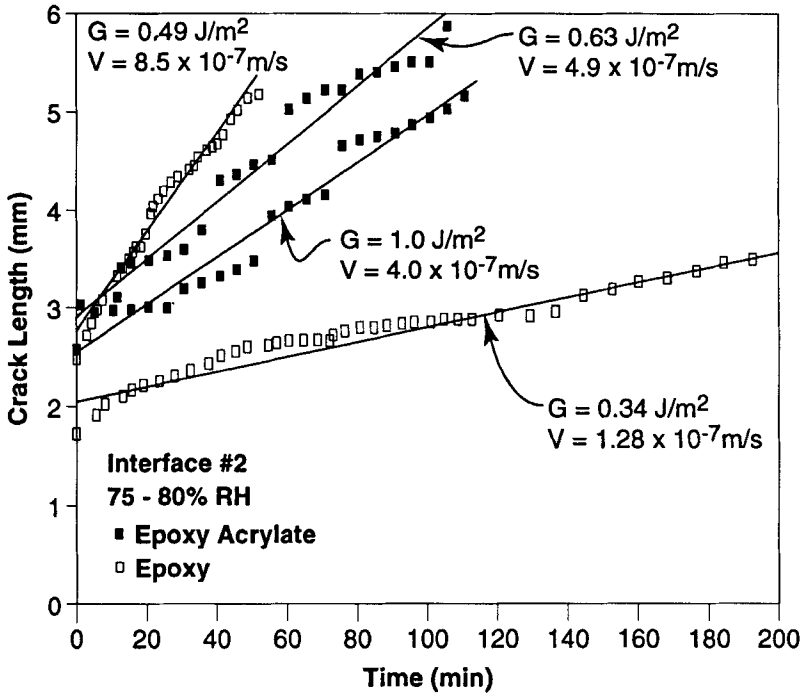
FIGURE 7   Crack length *versus* time for epoxy and epoxy-acrylate/glass sandwich specimens where cracks formed and grew exclusively on interface #2.

B. Finite Element Analysis

To provide a fundamental fracture mechanics background for understanding the experimental results of the various interfacial crack geometries, the interfacial, four-point flexure specimen was analyzed using the ABAQUS finite element program (Hibbitt, Karlson, and Sorenson, Inc.). For the finite element calculations, the elastic modulus and Poisson's ratio of the glass were taken to be 70 GPa and 0.30, respectively, and the corresponding values for the polymer adhesive were taken to be 2.8 GPa and 0.3. The 4-point flexure model overall dimensions were the same as the test apparatus and the thickness of the adhesive layer was generally 40 μm, except for a few cases where the thickness was varied from 20 to 160 μm to determine the effect of thickness on G and ψ. The applied load for all cases was $P = 2 N$. The characteristic length used to calculate the phase angle, ψ, was taken to be equal to the thickness of the adhesive layer.

In all cases, plane strain was assumed and symmetry at the center of the specimen at the midplane was imposed by constraining the x-displacement. For the specimens with cracks only on one interface, 8-noded isoparametric elements (CPE8) with 9 quadrature points were used. For the specimens with cracks on both interfaces, 4-noded isoparametric elements (CPE4) were used together with interface elements (INTER2) along the crack surfaces on both interfaces. Faster convergence of the solution was obtained using the CPE4 elements coupled with the interface elements. The interface
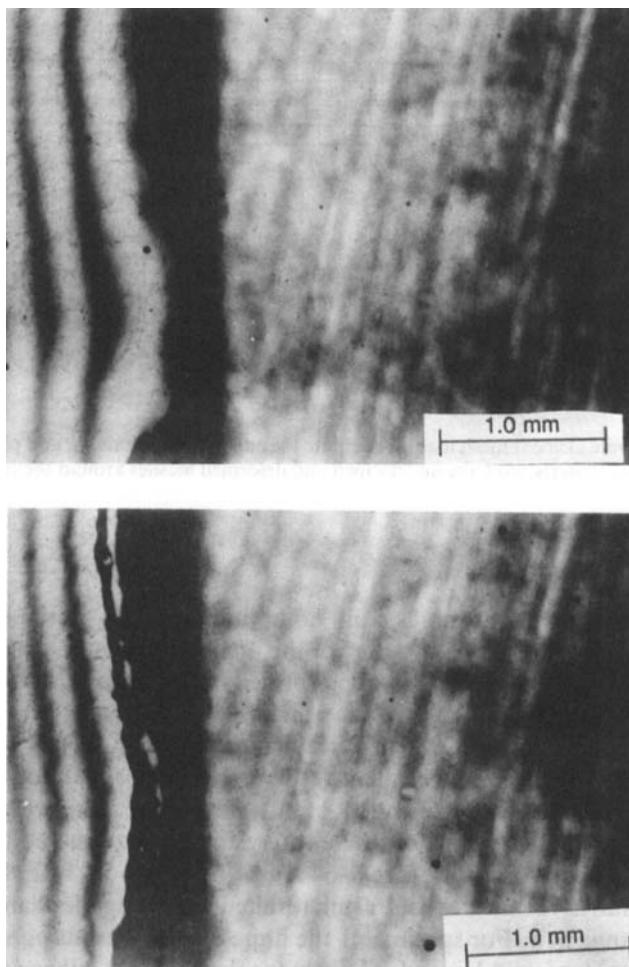
FIGURE 8   Micrograph of a crack receding on interface # 2 of an epoxy-acrylate/glass sandwich specimen at 75–80% RH and $G = 0.5 \, \text{J/m}^2$.

elements allowed the crack surfaces at the interface either to remain in contact without friction or to separate. For specimens with cracks only on one interface, approximately 2500 elements were used and about 4000 elements were used when cracks were on both interfaces. In the immediate vicinity of the crack tips, a ring of singular elements surrounded by 3 other rings of quadrilateral elements were generated to model accurately the crack tip singularity. These elements were approximately 0.5 μm on each edge.

Figure 9 shows the finite element mesh for a specimen with a crack on interface #1. An insert shows how the meshes at the crack tip are displaced under load. A concentrated load was used to model the load applied at the outer loading lines and a roller support was imposed at the inner loading lines. When the interface elements were
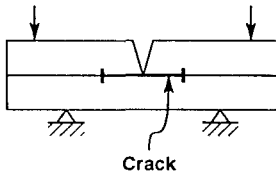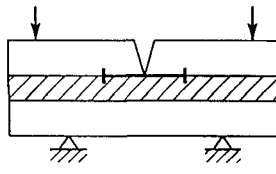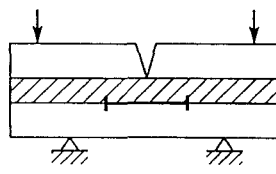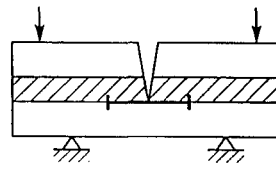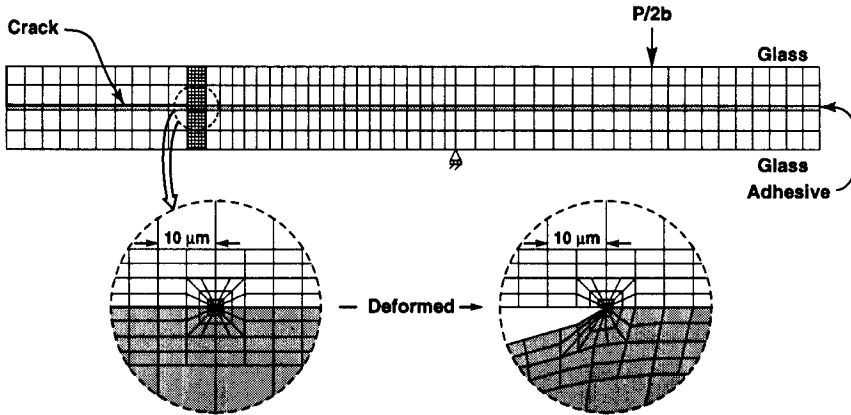
FIGURE 9   The finite element mesh used to compute the energy release rate, G, and phase angle, ψ, for a crack on interface #1. Inserts show the undeformed and deformed meshes around the crack tip.

used in the cases involving cracks on both interfaces, an initial crack opening displacement was prescribed at the start of the analysis to ensure convergence of the solution. The analysis in these cases was performed in two steps with a small fraction of the load applied initially, followed by the remainder of the load.

Table I summarizes the finite element results for specimens involving only a single interfacial crack. All these finite element results were independent of crack size from $a = 1.0$ to 4.75 mm and were independent of thickness of the adhesive layer from 20 to 80 μm. Specimen 4 was the most sensitive to the thickness of the adhesive and for a thickness of 160 μm, G decreased to 0.64 J/m^2 and ψ to 5°. For the other crack geometries, an adhesive thickness of 160 μm resulted in a negligible change in G and less than a 10% change in ψ. For specimen 1 the finite element results agree well with the analytical results[3] for a two-layered specimen (negligibly thick adhesive layer) as given by Eq. (1). Specimen 2 shows that the presence of a thin adhesive layer has a negligible effect on G but decreases ψ by 11°, in agreement with the asymptotic limit prediction of Suo and Hutchinson.[4] Comparison of specimen 2 and 3 shows that for the given applied load, G is reduced about 46% for an interfacial crack solely on interface #2, and the phase angle is reduced by 57%, indicating more of an opening mode of loading at the crack tip. Thus, the presence of the unbroken adhesive ligament limits the energy release rate for a given applied load and decreases the crack tip shear stress that tends to drive the crack out of the interface. The decrease in ψ indicates a more opening mode of loading at the crack tip and this would be expected to promote moisture-assisted crack growth since it would allow a larger accommodation for water molecules to displace the polymer adhesive at the glass interface. Specimen 4 shows that for cases when the adhesive layer is weak so that the initial crack penetrates through the adhesive layer before diverging into interface #2, the adhesive layer again has a negligible effect on G but now ψ is about twice that of specimen 2, in agreement with the asymptotic predictions of Suo and Hutchinson.[4] Although this crack geometry (specimen 4) was

TABLE I

Finite Element Analysis comparison of energy release rates (G) and phase angles (Ψ) for various test geometries of the four-point flexure sandwich specimen.

Specimen	G (J/m²)	Ψ
1	1.53	41°
2	1.55	30°
3	0.83	13°
4	1.55	55°

not observed in this research, the significant increase in ψ would be expected to inhibit moisture-assisted crack growth.

Tables II and III summarize the finite element results for specimens involving cracks on both interfaces #1 and #2. From Table II several important observations can be made relative to the dual crack growth observations discussed above. For no overlap of the two cracks, G for the crack on interface #2 is considerably less than that for the crack on interface #1 (G_1) and the ψ for the crack on interface #2 indicates the presence of considerable shear at the crack tips. Both of these effects would suggest that the crack on interface #1 would grow, leading to an overlap with the crack on interface #2. On the other hand, with overlap between the cracks on interface #1 and #2, G for the crack on interface #1 is now considerably less than the G for the outer crack tip on interface #2 (G_{20}) and ψ is greater. For the inner crack tip, G_{21} is much less than G_{20} and ψ_{21} indicates considerable shear at this crack tip. Thus, these finite element results correctly

TABLE II

Finite Element Analysis of energy release rates (G) and phase angles (Ψ) for different dual interfacial crack geometries of the four-point flexure sandwich specimen. The first subscript on G and Ψ refers to the interface and the second subscript refers to the inner and outer crack tip on interface #2
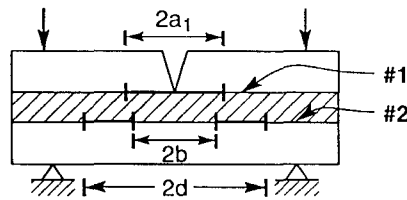
a₁ = 2mm and d = 4.75 mm

b (mm)	G_1	G_{2I} (J/m²)	G_{2O}	Ψ_1	Ψ_{2I}	Ψ_{2O}	
0.00	0.10	-	1.50	70°	-	54°	Overlap
0.75	0.14	0.06	1.41	70°	-70°	54°	Overlap
1.43	0.47	0.32	1.35	70°	-70°	54°	Overlap
2.26	2.54	0.98	0.04	43°	-74°	-76°	No Overlap
2.61	1.79	0.18	0.01	33°	-70°	-76°	No Overlap
3.25	1.57	0.02	0.00	30°	-70°	-70°	No Overlap
4.75	1.55	0.00	0.00	30°	-	-	No Overlap

predict the dual crack growth experimental observations discussed above. First, when cracks form on both interfaces #1 and #2, they always form with some degree of overlap. Second, the cracks on interface #2 do not grow toward the center of specimen but instead only the outer crack tip grows outward. Thirdly, crack growth on interface #1 is arrested once the crack on interface #2 becomes fully developed.

Table III expands the finite element results of Table II for a fixed overlap of $10t$ where t is the thickness of the adhesive layer. These results again confirm the above experimental observations and show that G_{2O} is relatively constant over a rather large range of crack sizes with a value about 10% less than that given by Eq. (1).

Based on these finite element results, the G values at the crack tips for the appropriate crack geometries were calculated as follows: for crack growth solely on interface #1, G was taken to be given by Eq. (1): for crack growth solely on interface #2, G from Eq. (1) was multiplied by 0.56 in accordance with the finite element results in Table I. For crack growth on interface #2 with a crack present on interface #1, the G calculated from Eq. (1) was reduced 10% based on the results in Table III.

TABLE III

Finite Element Analysis of energy release rates (G) and phase angles (Ψ) for different dual interfacial crack geometries of the four-point flexure sandwich specimen. The first subscript on G and Ψ refers to the interface and the second subscript refers to the inner and outer crack tip on interface #2
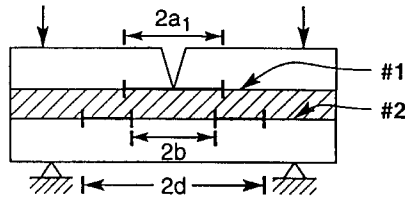

a_1 = 2mm and b = 1.6 mm

Overlap = 400 μm = 10 t

d (mm)	G_1	G_{2I} (J/m^2)	G_{2O}	Ψ_1	Ψ_{2I}	Ψ_{2O}
2.4	0.09	0.04	1.40	70°	-70°	54°
2.8	0.17	0.09	1.38	70°	-70°	54°
3.2	0.25	0.16	1.38	70°	-70°	54°
3.6	0.37	0.25	1.36	70°	-70°	54°
4.0	0.52	0.37	1.34	70°	-70°	53°
4.4	0.70	0.53	1.32	70°	-70°	53°
4.75	0.90	0.70	1.29	70°	-70°	53°

C. Crack Growth Rates

Figure 10 compares the moisture-assisted crack growth rates (velocity) of the epoxy specimens for crack propagation solely along either interface #1 or #2 (specimens 2 and 3 in Table I) to that for a crack growing on interface #2 in the presence of a crack on interface #1 (Table III). The threshold values of G, below which no crack growth was detected, are indicated by the data point with an arrow. Note that at the same value of G, velocities can vary by about an order of magnitude. This variability is thought to be related to both the intrinsic nature of moisture-assisted crack growth and batch-to-batch variability. Nevertheless, it is evident within experimental scatter that the crack growth rates for the different crack geometries are not significantly different. This variability was also seen in the threshold G values since there were some G values somewhat higher than the threshold values indicated on Figure 10 where with some samples the cracks grew and others where they did not. In any case, above the threshold G, all the crack growth rate data for the epoxy specimens can be fitted to a power law
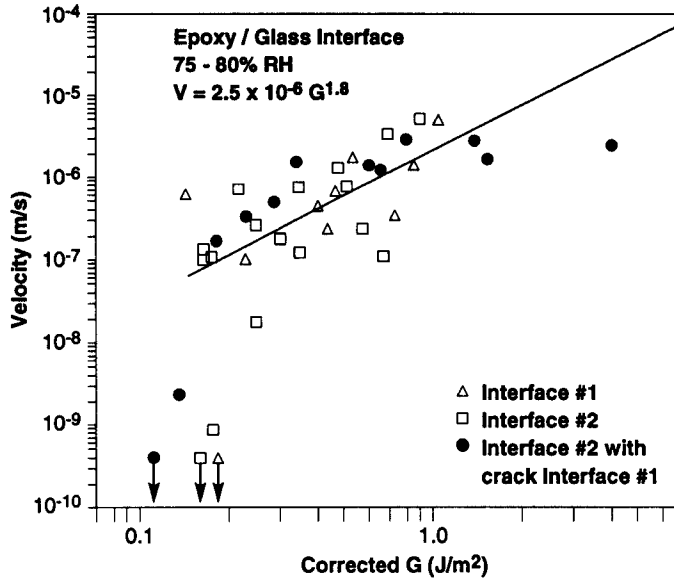
FIGURE 10   Comparison of the crack growth rates for the different crack geometries as a function of the corrected applied G for the epoxy/glass sandwich specimens at 75–80% RH.

relationship of the form

$$V = 2.5 \times 10^{-6} G^{1.8} \tag{2}$$

with a correlation (r) coefficient of 0.73. Equation (2) is shown as the solid line in Figure 10.

Moisture-assisted crack growth in the epoxy acrylate specimens was similar to that in the epoxy specimens as shown in Figure 11. Above a threshold value of G, crack growth rates were independent of the crack geometry within experimental scatter. The similarity of crack growth rates in samples with both interfaces smooth (S/S) to that where interface #1 is smooth and interface #2 is rough (S/R), indicates that the roughness of the interface opposite the interface where the crack is growing has an insignificant effect on the crack growth rate. Again, all the crack growth rate data were fitted to a power law relationship to give

$$V = 2.3 \times 10^{-7} G^{1.6} \tag{3}$$

with a correlation coefficient (r) of 0.78. Equation (3) is shown as a solid line in Figure 11. Comparison of Eqs. (2) and (3) shows that the power exponent, *i.e.* dependence of the crack growth rate on G, is similar for the two adhesives but that the crack growth rates for the epoxy-acrylate samples are an order of magnitude slower. The reason that the epoxy-acrylate/glass interface is more resistant to moisture-assisted crack growth than the epoxy/glass interface is not known since, according to manufacturer's data, the water absorption (%/24 h) of the epoxy is considerably less than that of the epoxy-acrylate (0.9 *vs.* 2.3). However, it should be noted that the epoxy-acrylate adhesive is considerably less stiff than the epoxy adhesive. The elastic modulus of the epoxy
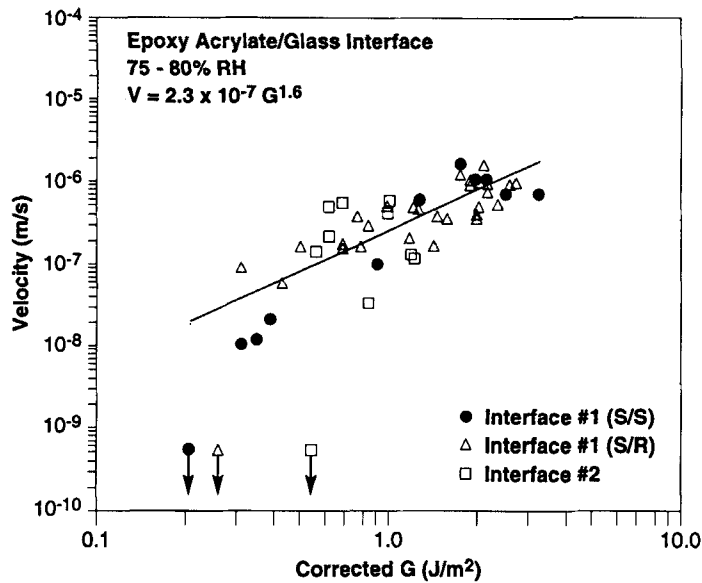
FIGURE 11   Comparison of the crack growth rates for the different crack geometries as a function of the corrected applied G for the epoxy-acrylate/glass sandwich specimens at 75–80% RH. Note that S/S refers to both glass interfaces being smooth and S/R refers to the glass interface #1 being smooth and interface #2 being rough.

acrylate is 0.65 GPa compared with 3.25 GPa for epoxy and the hardness of epoxy-acrylate is about 135 MPa compared with 200 MPa for epoxy.[1,5]

SUMMARY

In summary, it is believed that the agreement between the crack growth rates of the different crack geometries indicates that the primary driving force of moisture-assisted crack growth at epoxy and epoxy-acrylate/glass interfaces is the G at the crack tip. This agreement also implies that the phase angle differences between 13° (specimen 3 in Table I) and 54° (specimens in Table III) have a negligible effect on moisture-assisted crack growth. This latter result agrees with the results of Liechti and Chai[6] who measured no significant effect of phase angles from 0° to about 60° on the critical energy release rate (G_c) of an epoxy/glass interface.

Acknowledgment

References

1. K. M. Conley, J. E. Ritter and T. J. Lardner, "Subcritical Crack Growth Along Epoxy/Glass Interfaces," *J. Mater. Res.* 7 (9), 2621–2629 (1992).

2. J. E. Ritter, T. J. Lardner, G. C. Prakash, A. J. Stewart and V. Surova, "Dual Cracking at Polymer/Glass Interfaces," in *Adhesives Engineering*, SPIE Vol. **1999** (1993), pp. 80–86.
3. P. G. Charamlambides, H. C. Cao, J. Lund and A. G. Evans, "Development of a Test Method for Measuring the Mixed Mode Fracture Resistance of Bimaterial Interfaces," *Mech. Mater.* **8**, 269–283 (1990).
4. Z. Suo and J. W. Hutchinson, "Sandwich Test Specimens for Measuring Interface Crack Toughness," *Mater. Sci. & Eng.* **A107**, 135–43 (1989).
5. J. E. Ritter, D. R. Sioui, and T. J. Lardner, "Indentation Behavior of Polymer Coatings on Glass," *Polym. Eng. and Sci.* **32** (18), 1366–1371 (1992).
6. K. M. Liechti and Y. S. Chai, "Asymmetric Shielding in Interfacial Fracture Under In-Plane Shear," *ASME J. Appl. Mech.* **59**, 295–304 (1992).